Time-dependent focusing billiards and macroscopic realization of Maxwell's Demon

A B Ryabov[1] **and A Loskutov**[2,3]

[1] ICBM, University of Oldenburg, 26111 Oldenburg, Germany
[2] Physics Faculty, Moscow State University, Moscow 119899, Russia
[3] Institute of Physics, Humboldt University, Newtonstrasse 15, D-12489 Berlin, Germany

E-mail: a.ryabov@icbm.de and loskutov@chaos.phys.msu.ru

Abstract
The Fermi acceleration is always inherent in completely chaotic time-dependent billiards. At the same time, the particle dynamics in nearly integrable billiard systems can be more complex. Using a simplified approach, we investigate time-dependent stadium-like billiards and show that at a certain particle velocity, V_r, a resonance between external periodical perturbations and the motion within stability islands of the unperturbed billiard can be observed. This resonance suppresses the Fermi acceleration of particles with velocities less than V_r. As a result, we observe a separation of billiard particles by their velocities. If $V_0 < V_r$, the average particle velocity decreases, while the particles with $V_0 > V_r$ are on average accelerated. At the initial velocity $V_0 = V_r$ we observe a phase transition in the velocity distribution of particles: if $V_0 < V_r$ then the distribution approaches a stationary one, whereas for $V_0 > V_r$ the distribution is non-stationary and spreads toward the higher velocities. This phenomenon may be treated as a peculiar billiard Maxwell's Demon, when weak perturbations of a system lead the particle ensemble to separation. In other nearly integrable billiard systems similar resonances can lead to differences in the acceleration of particles with velocities smaller or larger than a resonance value.

PACS numbers: 05.20, 05.45

(Some figures in this article are in colour only in the electronic version)

1. Introduction

The analysis of the dynamics of billiard balls has been initiated by Coriolis [1] who, for the first time, theoretically studied billiards in a plane. Later Hadamard [2] examined a question about the particle motion on a twisted surface of negative curvature. However, the notion of
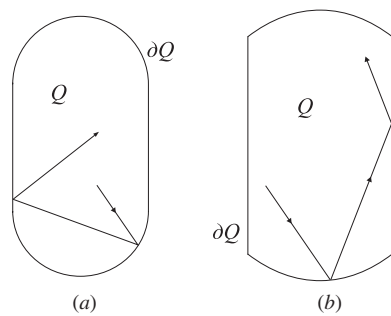
Figure 1. Stadium-like billiards.

billiards in the contemporary sense is known since Bikhoff [3] studied a problem of the free motion of a point particle (billiard ball) in a manifold. More complete investigation related to the mixing property in many-particle systems has been carried out by Krylov [4]. Later, thanks to the papers by Sinai [5] and then Bunimovich [6, 7] (see also [8]), the class of billiard problems has been essentially extended.

A billiard dynamical system is generated by the free motion of a point mass particle (billiard ball) in a region Q with a piecewise-smooth boundary ∂Q and by the condition of the elastic collision from ∂Q. If the boundary in the collision point is smooth, then the billiard ball reflects from it in such a way that the velocity tangent component remains constant, and the normal component changes its sign. Thus, in the Euclidean space, the incidence angle is equal to the angle of reflection. If the ball hits a corner of the billiard table, then its further motion is not determined.

If the billiard boundary consists of dispersing and neutral components, then such a billiard is said to be a dispersing one, or the Sinai billiard. One of the well-known dispersing billiards is the Lorentz gas [9]. On the basis of the analysis of a 2D Lorentz gas a remarkable result has been obtained that the dynamics of purely deterministic systems may be ergodic with mixing and similar to the Brownian motion [8].

The so-called focusing billiards include focusing components which can be connected by neutral ones. For some of such billiards one may prove that they possess the mixing property [7, 10]. The most known example of focusing billiards is 'stadium', or the Bunimovich billiards, which consist of two arcs and two rectilinear parallel segments joining them (figure 1). Quite general conditions of the chaoticity in 2D plane billiards are described in [11, 12] (see also references cited therein).

Billiards with boundaries, which oscillate according to one or another rule, represent a natural physical generalization of classical billiard systems. Indeed, the Lorentz gas has been proposed for the description of the motion of electrons between heavy ions in the lattice of metals. In reality, however, ions should weakly oscillate near their equilibrium state. Moreover, some important problems of mathematical physics can be described by non-stationary billiard models (see [13]). Thus, billiards with the time-dependent boundaries are a very interesting and important subject.

It is obvious that in time-dependent billiards the velocity of billiard particles changes from collision to collision. After a collision event the billiard particle gains or loses its energy depending on whether the billiard boundary is approaching (i.e. there is a head-on collision) or receding (i.e. there is a head–tail collision). Therefore, the investigation of the dynamics of the particle velocity becomes an important and interesting question: under what conditions on the billiard boundary acceleration and/or retardation of billiard particles will be observed?

For the first time the phenomenon of the particle acceleration by elastic collisions with massive moving obstacles has been considered by Fermi to explain the origin of high-energy cosmic rays [14]. Fermi argued that in a typical environment the probability of a head-on collision is greater than the probability of a head–tail collision, so particles would, on average, be accelerated. Later many approaches regarding the description of such a phenomenon were introduced for both the continuous and discrete time models (see [13, 15, 16] and references cited therein).

In this problem, dynamical properties of billiards play a principal role: if it possesses the chaotic behavior, then the boundary perturbation may lead to the particle acceleration. In papers [17, 18], on the basis of the analysis of chaotic billiards the following conjecture (known in the literature as LRA (Loskutov–Ryabov–Akinshin) conjecture, see e.g. [19–21]) has been advanced: a Fermi acceleration will be observed in time-dependent billiards if the corresponding fixed-boundary billiards exhibit chaotic properties. The matter is that in chaotic billiards the angle of incidence can be treated as a random value. Thus, the projection of the particle velocity onto the normal to the boundary is stochastic.

The LRA conjecture has been confirmed for the Bunimovich stadium [22], for annular billiards [23] and the time varying oval-shaped billiard [24]. Recently, using the theory of dynamical systems, it was proved that the Fermi acceleration should be observed in non-autonomous billiard-like systems [25, 26]. Finally, by applying thermodynamic methods it was shown [27] that the Fermi acceleration is inherent in the Lorentz gas of a quite general configuration.

Note, however, that this conjecture is a necessary condition, and it does not contradict to the emergence of the Fermi acceleration if the dynamics of some unperturbed billiards is integrable. For instance, the Fermi acceleration occurs in driven elliptical billiards [16, 28], because separatrices of an unperturbed elliptical billiard transforms into a chaotic layer if the boundaries are perturbed. As a result, in the perturbed elliptical billiard the particle motion can become chaotic even if all trajectories of the unperturbed case are regular.

It was also found that unexpected effects may be observed if the static billiard is a nearly integrable system [22]. In this case, all invariant curves in the phase space are surrounded by stochastic layers. Then, depending on the initial velocity value the particle ensemble in time-dependent billiards may be accelerated or decelerated.

This phenomenon can be treated as a specific (billiard) Maxwell's Demon. In 1871, Maxwell proposed a peculiar arrangement (Demon) which could select the gas of molecules containing in two chambers connected through a small hole. These chambers, following the second thermodynamics law, are at the equilibrium state. The Demon could hypothetically work against this law by separation of molecules by their velocities and the further chamber selection. The principal ideas concerning the Maxwell's Demon are presented in [29].

The physical realization of Maxwell's Demon for the fixed boundary billiards has been first proposed by Zaslavsky and Edelman [30, 31] (see also [32] and references cited therein). The authors considered two billiard tables connected through a hole and showed that this system does not reach equilibrium state even during extremely long period of time.

In the present paper we consider nearly integrable stadium-like billiards with periodically perturbed boundary and describe the origin of the increase and decrease of the particle velocity. The time dependence on the one hand complicates the particle dynamics, but on the other hand, gives conditions for the velocity separation of billiard particles. This makes it possible to suggest a macroscopic realization of Maxwell's Demon in nearly integrable time-dependent billiards when a weak boundary perturbation leads to the formation of two ensembles of slow and fast particles.
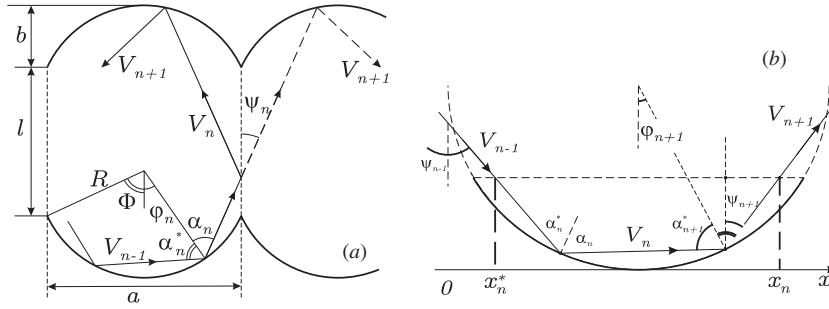
Figure 2. Coordinates in a stadium.

2. Stadium-like billiards

First let us describe the billiard models which are used in the present paper for simulations.

2.1. Billiards with fixed boundaries

Suppose that the focusing components are arcs of a circle of the radius R and of the angle measure 2Φ, and they are symmetrically placed with respect to the vertical billiards axis (figure 2(a)).

By a simple geometrical analysis we obtain the following relations:

$$R = \frac{a^2 + 4b^2}{8b}; \qquad \Phi = \arcsin \frac{a}{2R}.$$

Introduce the dynamical variables as shown in figure 2 and construct an exact map describing the particle dynamics in this billiard. We should consider two different cases.

- After a collision with a boundary the particle again collides with it (in other words, there is a series of collisions with the same boundary component, see figure 2(b)).
- The next collision occurs with another focusing component.

In the former case a geometric analysis [22] leads to the map

$$
\begin{aligned}
\alpha_{n+1}^* &= \alpha_n, \\
\alpha_{n+1} &= \alpha_{n+1}^*, \\
\varphi_{n+1} &= \varphi_n + \pi - 2\alpha_n (\mathrm{mod}\, 2\pi), \\
t_{n+1} &= t_n + \frac{2R \cos \alpha_n}{V_n}.
\end{aligned}
\tag{1}
$$

If $|\varphi_{n+1}| < \Phi$, then the billiard particle continues the series of collisions with the same boundary. Otherwise, the particle will collide with another focusing component and the corresponding map reads

$$
\begin{aligned}
\alpha_{n+1}^* &= \arcsin \left[\sin (\psi_n + \Phi) - \frac{x_{n+1}^*}{R} \cos \psi_n \right], \\
\alpha_{n+1} &= \alpha_{n+1}^*, \\
\varphi_{n+1} &= \psi_n - \alpha_{n+1}^*, \\
t_{n+1} &= t_n + \frac{R(\cos \varphi_n + \cos \varphi_{n+1} - 2 \cos \Phi) + l}{V_n \cos \psi_n},
\end{aligned}
\tag{2}
$$

where $\psi_n = \alpha_n - \varphi_n$, $x_n = [\sin \alpha_n + \sin(\Phi - \psi_n)]R / \cos \psi_n$, $x_{n+1}^* = x_n + l \tan \psi_n (\mathrm{mod}\, a)$.
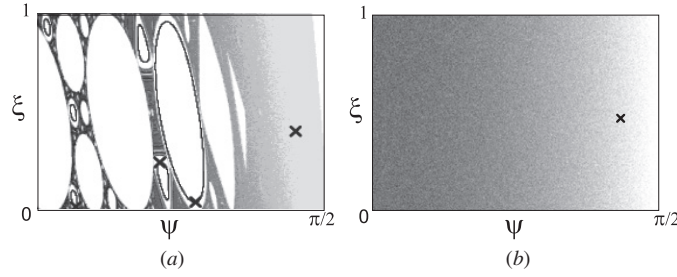
Figure 3. Phase portraits of stadium-like billiards generated by map (1) and (2). (*a*) Nearly integrable dynamics, $b = 0.01$. (*b*) Global stochasticity, $b = 0.25$. The black crosses mark initial conditions. Other parameters $l = 1$, $a = 0.5$; the trajectories which start in the stochastic area and in the regular regions include 5×10^8 and 10^7 iterations, respectively.

The particle dynamics in billiards, which have focusing components of a constant curvature, are chaotic if all these components complemented up to a circle, belong to the billiard table Q [10]. If $b \ll a$ this yields the stochasticity condition:

$$\frac{l}{2R} \approx \frac{4bl}{a^2} > 1. \tag{3}$$

It is convenient to represent the particle dynamics in the (ψ_n, ξ_n) coordinate plane, where ξ_n is the normalized horizontal coordinate of the collision point, $\xi_n = 1/2 + x_n/a$. Since the billiard has an axial symmetry, it is sufficient to consider results only for non-negative values of ψ. To plot the phase portrait we subdivide the available range into 300×300 cells and characterize the number of hits into a cell by the intensity of gray color. If b is small (the billiard shape is close to a rectangle), then the phase portrait contains islands of stability, which surround stable fixed points (figure 3(*a*)). Trajectories which start within such islands always stay on corresponding invariant curves. Furthermore, after a small perturbation of this trajectory, the billiard particle will proceed motion in a small neighborhood of the unperturbed trajectory. Thus, depending on the initial conditions, the phase point either randomly walks within the stochastic layer or rotates around a fixed point. With an increase of nonlinearity (i.e. of the parameter b) the fixed points lose their stability and the width of the stochastic layer grows. Ultimately, a global stochasticity area appears so that the whole phase space becomes accessible under any initial conditions (figure 3(*b*)).

2.2. Billiards with perturbed boundaries

Let us suppose now that the focusing components of the billiard boundary are perturbed periodically, $U(t) = U_0 f(\omega(t + t_0))$, where ω is the oscillation frequency. If the amplitude of billiard oscillations is sufficiently small, i.e. $U_0/\omega \ll l$, then we can neglect the boundary displacement with respect to the characteristic billiard size. In this approximation the billiard map reads
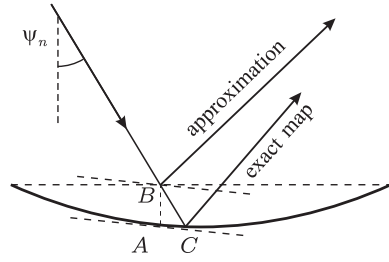
$$\begin{aligned}
V_n &= \sqrt{V_{n-1}^2 + 4V_{n-1}\cos\alpha_n^* U_n + 4U_n^2}, \\
\alpha_n &= \arcsin\left(\frac{V_{n-1}}{V_n}\sin\alpha_n^*\right),
\end{aligned} \tag{4}$$

$$\begin{aligned}
\alpha_{n+1}^* &= \alpha_n, \\
t_{n+1} &= t_n + \frac{2R\cos\alpha_n}{V_n}, \\
\varphi_{n+1} &= \varphi_n + \pi - 2\alpha_n \,(\mathrm{mod}\,2\pi),
\end{aligned} \tag{5}$$

Figure 4. The difference between the trajectories of billiard particles in the exact maps (1) and (2) and the approximated map (7).

if $|\varphi_{n+1}| \leqslant \Phi$, and

$$
\begin{aligned}
\psi_n &= \alpha_n - \varphi_n, \\
\varphi_{n+1} &= \psi_n - \alpha_{n+1}^*, \\
x_n &= \frac{R}{\cos \psi_n}[\sin \alpha_n + \sin(\Phi - \psi_n)], \\
x_{n+1}^* &= x_n + l \tan \psi_n (\mathrm{mod}\, a), \\
\alpha_{n+1}^* &= \arcsin\left[\sin(\psi_n + \Phi) - \frac{x_{n+1}^*}{R}\cos \psi_n\right], \\
t_{n+1} &= t_n + \frac{R(\cos \varphi_n + \cos \varphi_{n+1} - 2\cos \Phi) + l}{V_n \cos \psi_n},
\end{aligned}
\tag{6}
$$

if $|\varphi_n + \pi - 2\alpha_n| > \Phi$. Expressions (5) correspond to a series of successive collisions with one the same focusing component, and expressions (6) describe transition from one focusing component to another. Note that the only approximation that we used is the smallness of the boundary displacement.

3. Dynamics in the vicinity of stable points

In this section, we make an approximate analysis of a nearly integrable billiard configuration, when $l \gg a \gg b$. In this case, the circular arcs can be approximated by parabolas, and the fraction of successive collisions with the same boundary becomes negligible.

3.1. Billiards with fixed boundaries

Assume that the depth of focusing components is small enough. Then we can neglect the shift of a particle, when it moves within the circular arc. In other words (see figure 4), we will assume that the particle collides with the boundary at the point A (the projection of the point B onto the focusing arc), instead of the point C.

Under this assumption, the billiard map has a very simple form:

$$
\begin{aligned}
x_{n+1} &= x_n + l \tan \psi_{n+1} (\mathrm{mod}\, a), \\
\psi_{n+1} &= \psi_n - 2\beta(x_{n+1}),
\end{aligned}
\tag{7}
$$
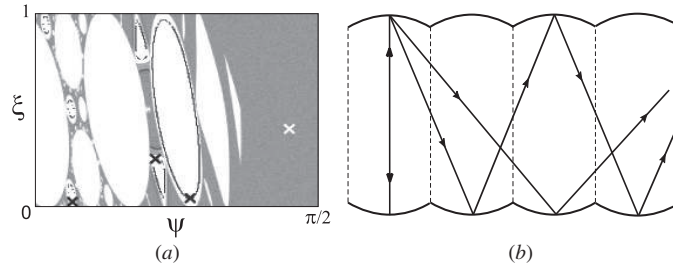
Figure 5. (*a*) The phase portrait of the stadium-like billiard system (8) with parabolic segments; parameters are the same as for figure 3(*a*). (*b*) Trajectories of the billiard ball which correspond to the main family of fixed points.

where $\beta(x) = \arctan \chi(x) \approx 4b(2x - a)/a^2$ is the slope of the focusing component at the point A. Introducing the normalized coordinate $\xi = x/a$, $\xi \in [0, 1)$ we obtain

$$\begin{aligned} \xi_{n+1} &= \xi_n + \frac{l}{a} \tan \psi_n (\mathrm{mod}\ 1), \\ \psi_{n+1} &= \psi_n - \frac{8b}{a}(2\xi_{n+1} - 1). \end{aligned} \tag{8}$$

On the one hand, this approach leads to a certain underestimation of the angle of reflection, if the angle of incidence ψ_n is a sufficiently large. As a result, the phase trajectories are nearly uniformly distributed in the stochastic layer, whereas for the exact map the region $\psi \approx \pi/2$ is almost empty (compare figures 3(*a*) and 5(*a*)). But on the other hand, when ψ is sufficiently small, this approach gives a quite good approximation of the billiard dynamics in the vicinity of fixed points. Thus, it makes possible to find the main family of such points: $\{\xi = 1/2,\ \psi_m = \arctan(ma/l)\}$, $m \in Z$. This family corresponds to the central fixed points of the largest stability islands (see figure 5(*a*)), and represents the trajectories shown in figure 5(*b*).

To analyze the stability of these points, let us linearize this map using new variables, which characterize the deviation of the trajectory from a fixed point m,

$$\Delta\xi_n = \xi_n - 1/2, \qquad \Delta\psi_n = \psi_n - \arctan(ma/l).$$

Then, assuming that this deviation is small enough and expanding map (8) into a series, we obtain

$$\begin{aligned} \Delta\xi_{n+1} &= \Delta\xi_n + \frac{l}{a \cos^2 \psi_m} \Delta\psi_n + O\left(\Delta\psi_n^2\right), \\ \Delta\psi_{n+1} &= \Delta\psi_n - \frac{16b}{a} \Delta\xi_{n+1}, \end{aligned}$$
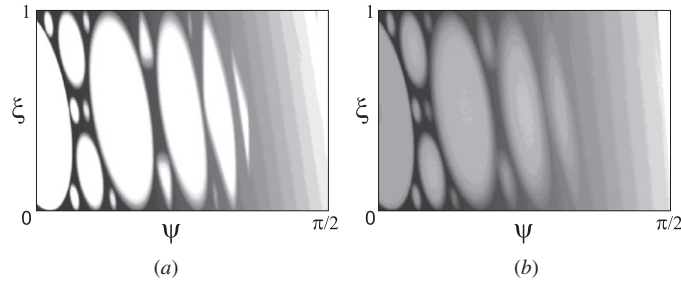
where $\psi_m = \arctan(ma/l)$. The corresponding transformation matrix has the form

$$A = \begin{pmatrix} 1 & \dfrac{l}{a \cos^2 \psi_m} \\ -\dfrac{16b}{a} & 1 - \dfrac{16bl}{a^2 \cos^2 \psi_m} \end{pmatrix}.$$

Since $\det A = 1$, this map preserves volume. From the stability criterion $|Tr A| \leqslant 2$ we get $\cos^2 \psi_m \geqslant 4bl/a^2$ or

$$m^2 \leqslant \frac{l}{4b} - \frac{l^2}{a^2}. \tag{9}$$

Figure 6. In a time-dependent billiard particles may penetrate into the stability islands of the unperturbed system: (*a*) the large particle velocity, $V \gg V_r$; (*b*) the resonance case, $V \approx V_r$. The parameter values for the maps (4)–(6) are the following: $l = 1$, $a = 0.5$, $b = 0.01$, $\omega = 1$, $U_0 = 0.005$.

Therefore, the transition to stochasticity takes place if $4bl/a^2 > 1$. Note that this expression coincides with condition (3).

Consider trajectory of a particle which moves around a stable fixed point m. Using the transformation into action-angle variables, one can show (see [22]) that this motion obeys a twisted map with the rotation number

$$\rho_m = \arccos\left(1 - \frac{8bl}{a^2 \cos^2 \psi_m}\right). \tag{10}$$

Because the time between two successive collisions can be estimated as

$$\tau_m \approx \frac{l}{\cos \psi_m} \frac{1}{V}, \tag{11}$$

the period of rotation is approximately equal to

$$T_{\rho_m} = \frac{2\pi}{\rho_m} \tau_m \approx \frac{2\pi}{\rho_m} \frac{l}{\overline{V} \cos \psi_m}, \tag{12}$$

where $\overline{V}$ is the average velocity during one period.

3.2. Boundary perturbations

Consider now a perturbed billiard with a weak nonlinearity of the focusing components. If the particle velocity is a large enough then the boundary perturbations have a small influence on the phase portrait (figure 6(*a*)). However, the period T_{ρ_m} of rotation around a fixed point depends on the particle velocity, while the period of the boundary oscillations $T_b = 2\pi/\omega$ is a constant. Thus, at a certain velocity $V = V_r$ these periods will be equal, and we will observe a resonance between boundary oscillations and rotation. At this velocity, due to the boundary perturbations the particle trajectory now can easily penetrate into the neighborhoods of fixed points and, moving along a spiral, first approaches the center and then leaves its neighborhood [22]. Furthermore, the rotation frequency remains the same as for the unperturbed billiard. As a result, the whole region turns out to be accessible (figure 6(*b*)).

Using equation (12) we obtain the value of the resonance velocity:

$$V_r = \frac{\omega l}{\cos \psi_m \arccos\left(1 - \frac{8bl}{(a \cos \psi_m)^2}\right)}. \tag{13}$$

This expression determines a set of resonance velocities $\{V_{r,1}, V_{r,2}, \ldots, V_{r,\max}\}$ which correspond to the fixed points with $m = 1, 2, \ldots, m_{\max}$. Note that because of the billiard
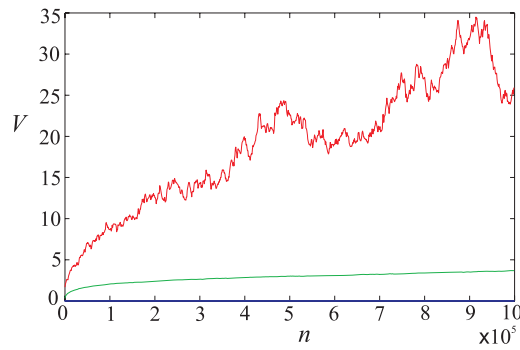
Figure 7. The average (green), minimal (blue) and maximal (red) velocities of an ensemble of 5000 particle as a function of the number of collisions in a stadium with fully chaotic dynamics (figure 1(a)). Parameters: $l = 2$, $a = 0.5$, $b = 0.25$, $U_0 = 0.01$, $\omega = 1$ and $V_0 = 0.1$.

symmetry, the resonance velocity at the central ($m = 0$) fixed point is two times smaller [22]. However, this resonance will not play an important role below, and we will always consider fixed points with $m \geqslant 1$.

## 4. Conditions of an increase or decrease of particle velocities

We carried out numerical simulations of maps (4)–(6) in two cases. In the first case we considered 'classical' fully chaotic billiards in the form of a stadium (figure 1(a)). In the second case we assumed that $l \gg a \gg b$ and investigated a nearly integrable billiard system (figure 1(b)).

For the fully chaotic billiards the average particle velocity was obtained for an ensemble of 5000 particles with different initial directions of the velocity vector. The trajectory of each particle has been calculated during 10^6 collisions with the billiard boundary.

Figure 7 shows the dependence of the average, maximum and minimum velocities in the ensemble of particles on the number of collisions. The average particle velocity (the central green curve) follows a power law $\overline{V}(n) \sim n^\gamma$, $\gamma = 0.44$. Thus, the Fermi acceleration phenomenon is inherent in this time-dependent billiard. To characterize the spread of particles we also plotted the minimal (the lower blue curve) and maximal (the red broken curve) velocity in the ensemble. The minimal velocity remains small (almost coincides with the abscissa axis) and fluctuates within the range $V_{\min} \in [10^{-5}, 3 \times 10^{-3}]$. The maximal velocity reached $V_{\max} = 34.5$ after 10^6 collisions.

The most intriguing behavior of the particle velocity we observe in nearly integrable billiards (figure 1(b)). In this case $b \ll l$, and the phase space of the system contains regions with regular and stochastic dynamics (figure 6). If the initial velocity of particles is sufficiently large then the average particle velocity grows, and the velocity distribution function becomes wider with the number of collisions (figure 8, top panel). If, however, the initial velocity is small enough, then the average particle velocity slows down up to a small value V_{fin}, and the particle distribution approaches to a stationary one with a relatively small variance (figure 8, bottom panel).

Note, however, that in the last case there is a small probability for particles to leave the region of small velocities. In particular, the maximal velocity of the ensemble grows (figure 8(c)). However, these events are rare and do not influence the particle distribution during the observation time, but their role can be crucial on an extremely long simulation
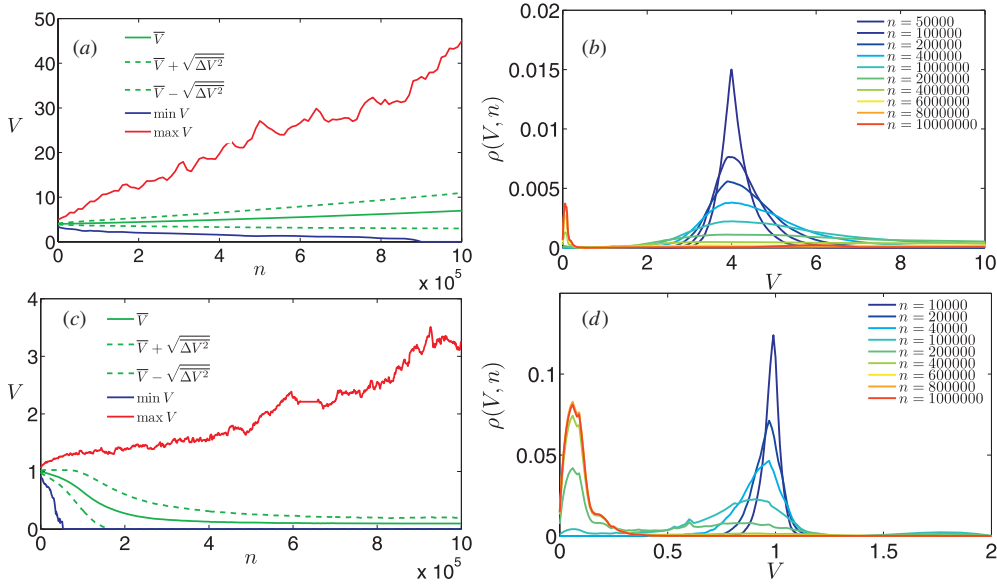
Figure 8. In time-dependent nearly integrable stadium-like billiards initially 'fast' particles will, on average, be accelerated, while the velocity of initially 'slow' particles decreases. (*a*) The dynamics of initially 'fast' particles, $V_0 = 4$. (*b*) The evolution of the velocity distribution function, corresponding to panel (*b*). (*c*), (*d*) The same for initially 'slow' particles, $V_0 = 1$. For each case an ensemble of 20 000 particles has been considered. For the parameter values see figure 6.

period. This is due to the fact that for 'fast' particles the probability of returning into the region of small velocities decreases with time because these particles will on average be accelerated, while the probability of leaving the small velocity region will be almost constant.

To find the velocity at which the particle separation occurs we investigated the width (standard deviation, $\sqrt{\overline{\Delta V^2}}$) of the particle velocity distribution after 10^7 collisions as a function of the initial velocity for different billiard parameters a and b (see figure 9). For calculations of each point we used an ensemble of 400 trajectories. This analysis shows that $\sqrt{\overline{\Delta V^2}}$ undergoes a first-order phase transition at a critical value V_c of the initial velocity. If $V_0 < V_c$ then the variance of the velocity distribution approaches to a small value. At the same time, $V_0 > V_c$ leads to a non-stationary distribution with an unlimited variance which grows with the number of collisions. Furthermore, the velocity distribution function (figure 8(*b*) and (*d*)) has a bimodal form with two maxima. This is an additional hint that we observe a first-order phase transition characterized by two attracting states.

We should make two comments here. Firstly, for some parameters values (e.g. for $b = 0.004$ and $b = 0.001$ in figure 9(*b*)) the particle separation is very slow and the number of steps 10^7 is not enough to clearly see it. As a result, these transitions look much smoother and resemble a second-order phase transition. However, analyzing the dynamics of velocity distribution functions, we still observe separation of particles into two groups with relatively high and low velocities.

Secondly, curves for $b \leqslant 0.002$ in figure 9(*b*) have a local maximum when V_0 is slightly larger than V_c. This maximum occurs due to the fact that for small b random fluctuations of the velocity diminish. As a result, the variance is relatively small if the initial velocity is large. If, however, the initial velocity is a little larger than V_c, then a fraction of particles, which are
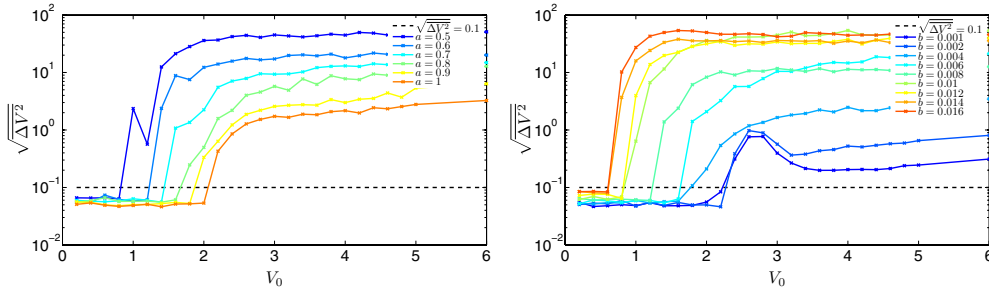
Figure 9. The standard deviation $\sqrt{\overline{\Delta V^2}}$ of the velocity distribution after 10^7 collisions as a function of the initial velocity plotted for different billiards parameters a at $b = 0.01$ (left panel) and b at $a = 0.5$ (right panel). The black dashed line shows a threshold value between narrow (the deceleration of particles) and wide (the acceleration of particles) distributions. Each data point is calculated for an ensemble of 400 particles. The other parameter values are the same as in figure 6.
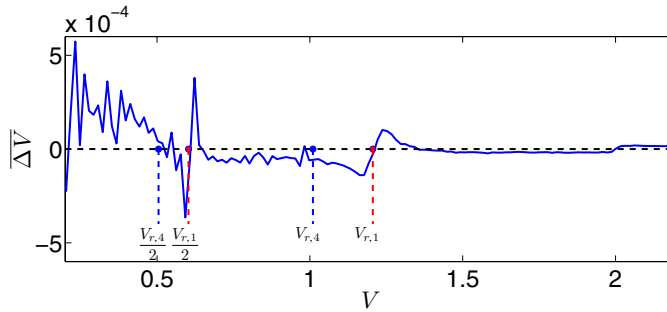
Figure 10. The average velocity change ΔV as a function of the particle velocity plotted for an ensemble of 20 000 particles with initial velocity $V_0 = 2$. The other parameters are the same as in figure 6. For these values $m_{\max} = 4$, and five stability islands exist.

decelerated and turn out to be trapped in a small velocity region, gives an essential additional impact in the variance. This leads to a local maximum of the variance at this value of the velocity.

We suppose that the critical velocity V_c is related to the resonance velocity V_r, and the transition in the velocity distribution occurs due to the differences in the dynamics of particles with smaller or larger than V_r velocities. In particular, we showed in [22] that when the particle velocity passes though the resonance value, the areas of acceleration and deceleration change their places in the phase space.

Furthermore, figure 10 shows that in the vicinity of $V_{r,1}$ (the resonance velocity in the stability island with $m = 1$) the average variation of the velocity $\overline{\Delta V}$ changes its sign. Similar resonance behavior appears at $V = V_{r,1}/2$.

To confirm this assumption we estimated the critical velocity from figure 9 as follows:

$$V_c \approx \frac{V_0^- + V_0^+}{2}, \tag{14}$$

where V_0^- is the last value of V_0 for which $\sqrt{\overline{\Delta V^2}}$ is less than a threshold value ($\sqrt{\overline{\Delta V^2}} = 0.1$, dashed black line in figure 9), and V_0^+ is the first value after which the variance becomes larger than $\sqrt{\overline{\Delta V^2}}$. Figure 11 compares the values of the critical velocity with the resonance velocities $V_{r,1}$ and $V_{r,\max}$ in the first and in the last stability islands, respectively. One can see
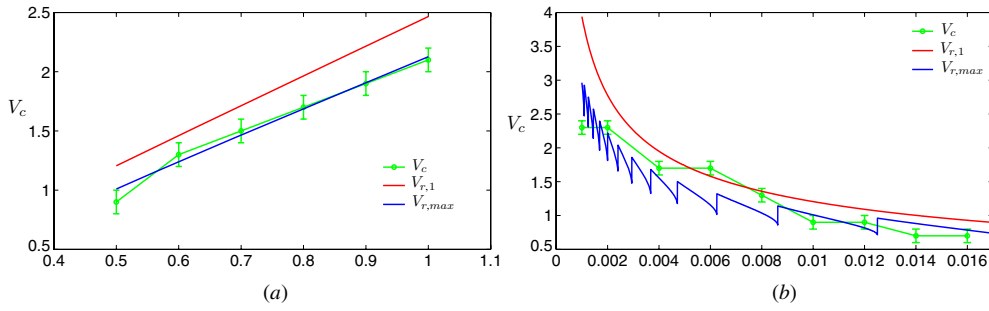
Figure 11. The critical velocity V_c as a function of the parameters a (left) and b (right) in comparison with the resonance velocities $V_{r,1}$ and $V_{r,\max}$ in the first and in the last islands of stability, respectively. The parameter values are the same as in figure 6.

that in a wide range of parameters the value of $V_{r,\max}$ (the minimal resonance velocity for a certain configuration) gives the best approximation of the critical velocity.

Note that the dependence of $V_{r,\max}$ on the parameter b is discontinuous and non-monotonic, because an increase of b leads to a decrease of V_r (see (13)), but at a certain value of b the last stable fixed point loses its stability, $m_{\max}$ decreases and $V_{r,\max}$ becomes larger. Note that the value of V_c also decreases non-monotonically with b.

5. Discussion

Thus, we have demonstrated that the presence of regular areas in the unperturbed billiard system can play an essential role in the dynamics of the particle velocity in the corresponding time-dependent billiard. This occurs due to a resonance between external perturbations and the motion within the stability islands which is inherent in the unperturbed system. This phenomenon may be observed in other two- and three-dimensional billiard systems, where similar resonance behavior can be found. However, it may not necessarily lead to the particle separation by their velocities. For instance, it can result in different acceleration rates of particles which move faster or slower than the resonance velocity.

In this section we will discuss some approximations of our modeling approach, show another possible way to determine the critical velocity and present a heuristical explanation of the particle separation by velocities.

First, in the considered system the presence of infinitely heavy walls plays a crucial role. Deceleration of particles ('cooling') and their acceleration ('heating') occur because the particle energy is either absorbed by the billiard boundary at head–tail collisions, or grows as a consequence of head-on collisions. Thus, we assume that in this system collisions of particles with the infinitely heavy billiard walls change only the particle energy and do not change the energy of the boundaries. This can be interpreted as a work of some external forces.

Second, note that for the derivation of the billiard map (4)–(6) we used the fixed boundary approximation. This approximation is widely used in the analysis of perturbed billiards [23, 33] and goes back to the classical papers of Lichtenberg and Lieberman (see [15]). However, recently it was found [16, 34] that such an approach leads to systematic underestimations of the velocity increment. Therefore, it is important to compare the described relations with the results obtained for an exact model where the boundary displacement is not neglected [35].

Consider now an alternative way to find the critical velocity. In the main part of the present paper we concentrated on the analysis of the variance of the particle velocity distribution after
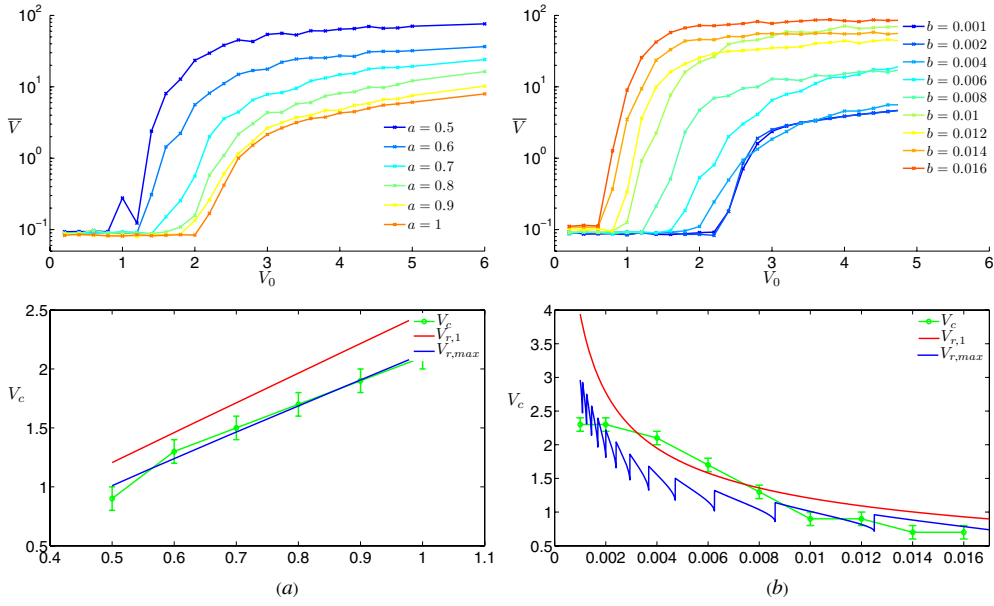
Figure 12. Top panel: the average velocity of an ensemble of 400 particles after 10^7 collisions as a function of the initial velocity plotted for different values of a at $b = 0.01$, and b at $a = 0.5$. Bottom panel: the critical velocity V_c based on $\overline{V}_{\text{fin}}$ after 10^7 collisions (compare to figure 11). The parameter values see in figure 6.

an essential number of steps. However, similar calculations can be performed for the average velocity $\overline{V}_{\text{fin}}$ of an ensemble of particles after a large number of steps. The top panel in figure 12 shows that this value also undergoes a phase transition.

The critical velocity may be defined as the velocity at which the function $\overline{V}_{\text{fin}}(V_0)$ starts to grow after a plateau. To determine this value numerically we used the first pair of initial velocities V_0^- and V_0^+, for which $\overline{V}_{\text{fin}}(V_0^+) - \overline{V}_{\text{fin}}(V_0^-) > \Delta_{\text{th}}$, where the threshold value Δ_{th} should be large enough to distinguish noise from monotonic growth (we used $\Delta_{\text{th}} = 0.015$). Calculating the critical velocity according to (14), we obtain very close values (compare with figure 11 and the bottom panel in figure 12).

So far we have discussed only numerical evidence of the particle separation by velocity. Now we turn to a possible explanation of this phenomenon. To understand the origin of the particle separation we should more carefully consider the particle dynamics in the vicinity of fixed points.

The phase portrait of a nearly integrable billiard configuration with the fixed boundary consists of stochastic layers and stable fixed points surrounded by stability islands (figure 3(*a*)). In the vicinity of a fixed point the particle motion can be represented as rotation around this point with a certain period T_{ρ_m}, see equation (12). All trajectories are located either on the elliptical invariant curves or in the stochastic layer and the particle cannot move from one invariant curve to another or to the stochastic layer.

In contrast, in time-dependent billiards the whole phase space may become accessible (figure 6). However, after a head-on collision the particle trajectory can enter into a stability island only from the right side in figure 6, because an increase of the particle velocity leads to a smaller angle of reflection and shifts the particle trajectory to the left in comparison with the trajectory in the absence of perturbations. Similarly, a decrease of the velocity allows entering only from the left side of an island of stability. This mechanism synchronizes the

phases of rotation around fixed points and periodic perturbations. If the phase difference is small enough and both periods are close to each other, we observe the resonance behavior: the particle follows a spiral trajectory approaching the fixed point and leaves its neighborhood when the phase difference becomes large.

There is an essential difference in the dynamics of velocity of particles moving within the stochastic layer and within the stability islands. In the stochastic area, the angles of incidence can be large and the flights between collisions can be long, while in the regular area successive collisions occur almost at the same incidence angles and in regular intervals of time. As a result, in the stochastic area the velocity changes more chaotically and slower than in the vicinity of fixed points. In particular, detailed analysis shows that the average change of velocity vanishes in the stochastic area, while there are areas of acceleration and deceleration within the stability islands [22]. Note that this is true only if the particle can occasionally enter and leave regular regions. If, however, a particle moves along an invariant curve of the perturbed system, then the change of total velocity tends to zero.

To get an insight into the mechanism of the particle separation by their velocities, consider a particle with $V < V_r$. The particle enters into the vicinity of a fixed point if the phases of rotation and boundary oscillations are close to each other. Since $V < V_r$, the rotation around the fixed point will be slower, and the phase delay will increase. Finally, the particle will return in the stochastic area. However, if the particle enters the regions of regular motion at the phase when it decelerates due to collisions with boundaries, then the phase delay will increase even faster, and the particle can leave this area after only a few head–tail collisions, which decrease its velocity. At the same time, if the particle initially accelerates in the regular region, then the phase delay will increase slower, and the particle can stay in this area longer. As a result, the velocity growth will be compensated by a further velocity decrease. Similar ideas show that a particle with $V > V_r$ will rather have accelerating collisions and then return to the stochastic area. We believe that this mechanism breaks the symmetry and leads to the separation of particles by their velocities.

6. Conclusion

The dynamics of the particle velocity crucially depends on the shape of stadium-like billiards. If the shape is close to a classical stadium (the nonlinearity parameter b is large enough), then the average velocity of a particle ensemble grows so that the Fermi acceleration takes place. The same acceleration is inherent in other chaotic billiards (see introduction). At the same time for the nearly integrable case a particle separation can be observed: there is a critical value V_c such that if the initial velocity $V_0 < V_c$, then the average velocity of the particle ensemble decreases up to a small (non-zero) value. However, if $V_0 > V_c$, then the particle velocity increases infinitely. In a certain sense this phenomenon can be considered as a specific (billiard) Maxwell's Demon, when by means of weak perturbations of the system we may sort fast and slow particles.

The physical nature of the particle separation lies in a resonance between boundary oscillations and the quasi-periodical motion in the vicinity of a fixed point. Similar resonance phenomena can be observed in other billiard systems (e.g. in elliptical billiards) where one time scale occurs in the unperturbed system because of the particle motion along a quasi-periodic stable trajectory, and another time scale is given by an external perturbation. The first time scale decreases with the particle velocity as $\sim 1/V$. Thus, at a certain velocity V_r both time scales should be equal and we will observe a resonance. Furthermore, a set of periodical orbits may lead to a set of essentially different resonance velocities. It is not necessary that these resonances will lead to the separation of particles by their velocities, but they can

result in a different character of the velocity change for the particles with smaller and larger velocities.

In addition, in our analysis we used the fixed boundary approximation. Therefore, it is important to compare the described phenomena with the results obtained for exact models of time-dependent nearly integrable billiard systems [35].

Acknowledgments

References

[1] Coriolis G-G 2005 *Mathematical Theory of Spin, Friction, and Collision in the Game of Billiards* Engl. Transl.
[2] Hadamard J 1898 *J. Math. Pures Appl.* **4** 27
[3] Birkhoff D 1927 *Dynamical Systems* (New York: American Mathematical Society)
[4] Krylov N 1979 *Works on the Foundations of Statistical Physics* (Princeton, NJ: Princeton University Press)
[5] Sinai Ya G 1970 *Russ. Math. Surv.* **25** 141
[6] Bunimovich L A 1974 *Funct. Anal. Appl.* **8** 73
[7] Bunimovich L A 1979 *Commun. Math. Phys.* **65** 295
[8] Bunimovich L A and Sinai Ya G 1981 *Commun. Math. Phys.* **78** 479
[9] Cornfeld I P, Fomin S V and Sinai Ya G 1982 *Ergodic Theory* (Berlin: Springer)
[10] Bunimovich L A 1991 *Chaos* **1** 187
[11] Tabachnikov S 2005 *Geometry and Billiards* (New York: American Mathematical Society)
[12] Chernov N and Markarian R 2003 *Introduction to the Ergodic Theory of Chaotic Billiards* (Rio de Janeoro, Brazil: IMPA)
[13] Loskutov A 2007 *Phys.-Usp.* **50** 939
[14] Fermi E 1949 *Phys. Rev.* **75** 1169
[15] Lichtenberg A J and Lieberman M A 1992 *Regular and Chaotic Dynamics* (Berlin: Springer)
[16] Karlis A K, Papachristou P K and Diakonos F K 2007 *Phys. Rev.* E **76** 016214
[17] Loskutov A, Ryabov A B and Akinshin L G 1999 *J. Exp. Theor. Phys.* **89** 966
[18] Loskutov A, Ryabov A B and Akinshin L G 2000 *J. Phys. A: Math. Gen.* **33** 7973
[19] de Carvalho R E, Souza F C and Leonel E D 2006 *Phys. Rev.* E **73** 066229
[20] Livorati A L, Ladeira D and Leonel E D 2008 *Phys. Rev.* E **78** 056205
[21] Lenz F, Diakonos F K and Schmelcher P 2008 *Phys. Rev. Lett.* **100** 014103
[22] Loskutov A and Ryabov A 2002 *J. Stat. Phys.* **108** 995
[23] de Carvalho R E, de Sousa F C and Leonel E D 2006 *J. Phys. A: Math. Gen.* **39** 3561
[24] Leonel E D, Oliveira D F M and Loskutov A 2009 *Chaos* **19** 033142
[25] Gelfreich V and Turaev D 2008 *J. Phys. A: Math. Gen.* **41** 212003
[26] Gelfreich V and Turaev D 2008 *Commun. Math. Phys.* **283** 769
[27] Loskutov A, Chichigina O and Ryabov A 2008 *Int. J. Bifurcation Chaos* **18** 2863
[28] Lenz F, Petri C, Koch F N R and Schmelcher P 2009 *Complex Phenomena in Nanoscale Systems* (*NATO Science for Peace and Security Ser. B: Physics and Biophysics*) ed G Casati and D Matrasulov (Berlin: Springer) p 209
[29] Leff H S and Rex A (eds) 1990 *Maxwell's Demon* (Princeton, NJ: Princeton University Press)
[30] Zaslavsky G M and Edelman M 1997 *Phys. Rev.* E **56** 5310
[31] Zaslavsky G M and Edelman M A 2004 *Physica* D **193** 128
[32] Zaslavsky G M 2005 *Hamiltonian Chaos and Fractional Dynamics* (Oxford: Oxford University Press)
[33] Leonel E D, McClintock P V E and da Silva J K L 2004 *Phys. Rev. Lett.* **93** 014101
[34] Karlis A K, Papachristou P K, Diakonos F K, Constantoudis V and Schmelcher P 2006 *Phys. Rev. Lett.* **97** 194102
[35] Loskutov A, Ryabov A B and Leonel E D in preparation